Multi-Layer Printed Shear Force Sensor on Flexible Substrates

Andreas Albrecht, Mauriz Trautmann, Markus Becherer, and Almudena Rivadeneyra
Institute for Nanoelectronics
Technical University of Munich
Munich, Germany
e-mail: Andreas.Albrecht@tum.de

Paolo Lugli
Free University of Bozen-Bolzano
Bozen-Bolzano, Italy
e-mail: Paolo.lugli@unibz.it

***Abstract*— Printed electronics technology is a promising way of fabricating low-cost electronics without the need for masking and etching. In recent years, additive printing techniques, such as inkjet and screen printing, have been adopted to fabricate low-cost and large-area electronics on flexible substrates. In this work, the design of a 3-axial normal and shear force sensor was developed, that consists of four miniaturized printed capacitors. The partially overlapping electrodes are arranged in a manner so that force sensitivity in orthogonal directions is achieved. The base unit of this sensor has been fabricated using inkjet-printing and characterized. The force response of this sensor was investigated in a force range from 0.1 N to 8 N, the normal-force sensitivity was determined to be S_z = 5.2 fF/N and the shear-force sensitivity was S_y = 13.1 fF/N. Due to its sensing range, this sensor could be applicable in tactile sensing systems.**

Keywords-Capacitive sensor; inkjet printing; normal force; PDMS.

I. INTRODUCTION

Printed electronics possess the advantage to reduce the number of production steps by applying several components with similar process technologies. In contrast to conventional electronics, sensors can be printed instead of assembled. The present work deals with the development, fabrication, and characterization of a capacitive normal and shear force sensor. Such sensors could be used for basic force and pressure measurements. They could also be part of a tactile sensing system in robotics. Advanced robotic systems need reliable information about friction and strain when interacting with the environment and handling objects [1]. Additionally, the ability of printed electronics to fabricate devices on flexible substrates could bring us a step closer to an artificial skin, which can be wrapped around the robot surface [2].

In a previous work, we studied inkjet printing and photonic sintering for low-cost printing of electrodes and wiring [3]. Chase et al. [4] showed a parallel plate capacitor approach with four capacitances that change in the overlapping area for exposure to shear forces and in distance for normal forces. Khan et al. [5] presented an all screen printed flexible pressure (normal force) sensor with a piezoelectric sensing principle. Silver (Ag) based paste serves as a conductor, and the piezoelectric material was polyvinylidene fluoridetrifluoroethylene (P(VDF-TrFE)), which is a ferroelectric polymer that exhibits efficient piezoelectric and pyroelectric properties. The force response was characterized by the voltage readout.

A thin-film normal and shear force sensor was designed by Chase and Luo [4]. Their capacitive device senses normal and shear forces simultaneously. The operation is based on the deflection of a compressible filler material, which is sandwiched between two electrodes of a plate capacitor. Making a few adjustments, this design could be implemented using printing technologies. A more advanced sensor design was reported by Dobrzynska and Gijs [6] using conventional semiconductor technology. Their capacitive approach is based on the deflection of an elastic dielectric spacer. Especially for shear force sensing, they used multiple small capacitor areas leading to a higher sensitivity. However, the fabrication of similarly small features is a challenging task using printed-electronics techniques.

In the present work, the basic idea of their sensor was adopted for printed electronics. The rest of the paper is structured as follows. In Section 2, we present the materials, the printing process, the elastic dielectric and its application as well as the characterization tools used to produce the presented results. Section 3 discusses the design, a theoretical model thereof as well as the evaluation of the print quality and the measured electromechanical behavior of out sensors. In Section IV, we summarize the main findings and conclude the paper.

II. MATERIALS AND METHODS

A. Materials

The shear-force sensors were fabricated on the transparent coated Polyethylene Terephthalate (PET) film Screenfilm Waterbased (Colorgate Digital Output Solutions GmbH, Germany). The film was developed for inkjet printing and has a nano-porous surface coating and has a grammage of 210 g m^{-2} and a thickness of 170 µm.

For inkjet printing, we used the nanoparticle-based silver ink DGP 40LT-15C (ANP Co., South Korea). The ink contains 35 % silver nanoparticles dispersed in TGME ($C_8H_{18}O_4$), which is a polar solvent. The dispersion was carefully shaken by hand prior to filling into the cartridge. The curing temperature is indicated with 120 – 150 ºC and the specific resistivity is 11 - 12 µΩ cm. As the dielectric spacer of our sensor, we used a two-component screen-printable silicone paste, Alpatec 30191 (CHT R. Beitlich GmbH). The

 ISBN: 978-1-61208-621-7

two components were mixed equally (1:1) in a small dish. After mixing, the paste can be used for one hour before hardening. Both components are highly transparent.

B. Inkjet-printed electrodes

The printer used in this work is a Dimatix DMP-2850 (Fujifilm Dimatix Inc., Santa Clara, USA). The cartridge and plate temperature was set to 55ºC with a drop-spacing of 30 µm. With these settings, the fabrication of one electrode took about ten minutes. By using more than one nozzle, the printing time can be reduced, but the probability of a failure due to a blocking in one of the nozzles is much higher. Through the heat of the platen, the pattern was quickly dried. To make sure that all the solvents evaporated, the samples were additionally cured in an oven for 60 min at 60 ºC.

To improve the conductivity of the electrodes, we employed Intense Pulsed Light (IPL) sintering using a Sinteron 2010 (Xenon, US). A double pulse (period of 3 s) at 2.5 kV was used. The pulse lengths were 500 µs for the first pulse and 1000 µs for the second pulse, which was identified as a good value in previous work [3]. The manufacturer measured a light intensity of 2.6 - 3.28 J mm^{-2} for a single pulse at 830 J.

C. Elastic spacer

The Polydimethylsiloxane (PDMS) spacer was applied onto the inkjet-printed silver layer on the PET film using a stencil made of 75 µm thick Kapton film. After applying PDMS on both electrodes, they were placed on each other, aligned using alignment marks and baked on a hot plate at 60 ºC for about 30 min. To make sure that the electrodes did not detach, a slight pressure was exerted on the sample using a glass slide. In this way, we effectively used the PDMS both as an adhesive as well as a dielectric spacer of our sensor.

D. Characterization

Optical microscope images were taken with a Zeiss Germany Axio.Lab A1, equipped with a digital camera Axiocam 105. These images were used to assess the quality of the printed electrodes and to determine their lateral and longitudinal dimensions. Further, the drop diameter of the silver ink on the PET and Kapton substrate were identified.

The thickness of our printed electrodes and PDMS layer were measured with a DektakXT stylus surface profiler (Brucker Corporation, USA).

To generate the normal and shear force, we used the voice coil linear actuator V-275 PIMag (Physikinstrumente, Germany) with an integrated force sensor. Figure 1(a) shows the actuator mounted to a movable stage for the normal force application. The fabricated sensor was fastened to the table using double-sided adhesive tape. To reduce parasitic capacitive coupling, a 2.5 mm x 2.5 mm glass slide was put between the metallic bar of the motor and the sensor. The capacitance of a fabricated sensor was continuously monitored using an Agilent E4980A Precision LCR Meter(100 kHz, 0 V bias, 1 V AC voltage). The characterization was automated by a LABVIEW program.

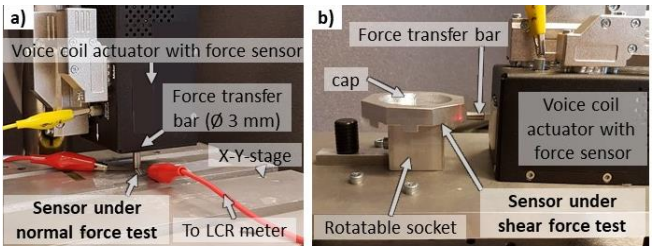

Figure 1. Measurement setup for (a) normal forces and (b) shear forces. The metallic bar transfers the force generated by the voice coil actuator to the sensor and the cap where the sensor is fixed, respectively.

For the shear force characterization, a different setup was developed and built using the same voice coil actuator. Figure 1(b) shows the measurement setup. The force is applied precisely on the sensor plane, thus parasitic forces are minimized. To characterize the samples from all directions, the socket can be rotated from -90 to +90. One side of the sensor is fixed (double-sided tape) to the socket and the other side to the cap. To route the wiring out, small grooves are milled into the bottom of the cap.

For the electro-mechanical characterization, we loaded the sensors with forces from 0.1 N to 8 N with incremental steps of 20 % every five seconds, and subsequently, the force was reduced by the same factor. This was repeated three times. The time-force-signal is shown in Figure 2. For evaluation of the hysteresis, we differentiated between the rising and the declining edges of the profile. In the following, the rising edges are labeled with R and the declining edges are denoted with D.

III. Results and Discussion

A. Sensor design

The design of the sensor was defined by the requirements and technical capabilities described in the previous sections. Thus, we were looking for a sensor, which can be fabricated on flexible substrates, like Kapton and PET using inkjet and screen printing. In literature, different capacitive sensors were demonstrated. For example, Chase et al. [3] presented a shear and normal force sensor where four squared electrodes form the bottom and a single squared electrode the top of the sensor. The operation was based on the deflection and compression of the filler layer between top and bottom electrodes.

The shear force and direction were then determined by calculating the ratios of the four single capacities. The

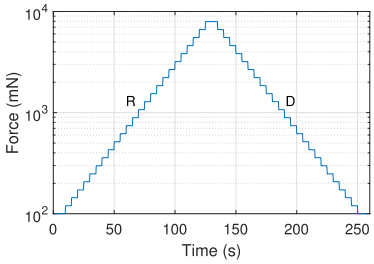

Figure 2. Force profile for normal and shear response measurements with increasing (R) force from 100 mN in steps of 20 % up to 8 N and decreasing (D) force with the same values.

downside of this configuration is that one only obtains very small delta in the capacity, especially when measuring shear force. Therefore, the basic principles of the four individual capacitors had to be modified to achieve an improvement in sensitivity.

So, instead of using square electrodes, we chose an 'E'-shaped pattern for both the top and the bottom electrode. This approach was firstly presented by Dobrzynka and Gijs in 2013 [4]. Figure 3 shows the proposed design of our sensor. The benefit of these 'E'-shaped structures is that one obtains multiple edges, so that a deflection leads to a change in the parallel area of the capacitor. The top and bottom electrode are displaced by half of the finger width, so the initial capacity amounts to 50% of the maximum capacity. Two of the capacitors are x-axis-sensitive, and the other two are y-axis sensitive.

B. Theoretical Model

The sensor was modeled using a simple parallel-plate capacitor approach according to (1). The design of the sensor uses identical areas A and distances d of the parallel plates for all capacitances in the relaxed position with no applied force.

$$C_0=\varepsilon_0\varepsilon_r\frac{A}{d} \tag{1}$$

A force in z-direction reduces the distance by Δd_z, thus, increasing the capacitance of all capacitances. The design of the sensor assures that an x-force increases the area ΔA_x of C_1 to the same extent it reduces the area of C_3 according to (2) and does not influence C_2 and C_4. Similarly, a y-force increases the area of C_2 and decreases the area of C_4 by ΔA_y.

$$C_{1/3}=\varepsilon_0\varepsilon_r\frac{A\pm\Delta A_x}{d-\Delta d_z} \qquad C_{2/4}=\varepsilon_0\varepsilon_r\frac{A\pm\Delta A_y}{d-\Delta d_z} \tag{2}$$

The average of all the capacitor values cancels out all area changes due to x- and y-forces and, thus, only depends on the change of the distance of the parallel plates. The z-force can be determined by the change of C_z.

$$C_z=\frac{1}{4}\sum_{n=1}^{4}C_n=C_0\cdot\frac{d}{d-\Delta d_z}\approx C_0\cdot\left(1+\frac{\Delta d_z}{d}\right) \tag{3}$$

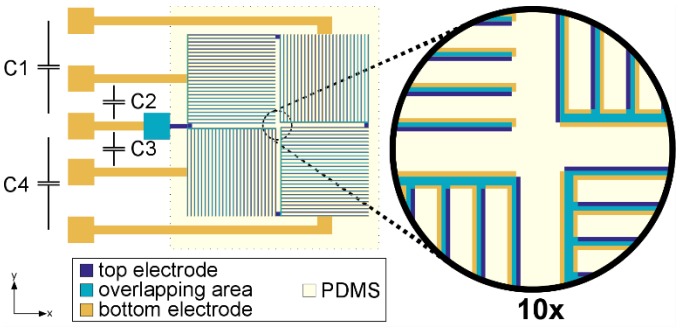

Figure 3. Design of our sensor with the four sectors that form the four capacitances C1 ... C4 that allow the differentiation of forces in x-, y- and z-direction. In every sector, the top and bottom electrode is shifted in a different direction.

A shear force exerted in positive x-direction causes an increase in capacity C_1 and a decrease of C_3 and can be expressed by (4).

$$C_{1/3}=\left(1\pm\frac{\Delta A_x}{A}\right)\cdot C_z \tag{4}$$

A subtraction of these two capacitances leads to an expression that reduces the z-dependence and can serve as an indicator for the applied x-force. Similarly, an expression for the
y-force can be derived from C_2 and C_4 that remain constant for any x-force.

$$C_x=\frac{(C_1-C_3)}{2\cdot C_z}=\frac{\Delta A_x}{A} \qquad C_y=\frac{(C_2-C_4)}{2\cdot C_z}=\frac{\Delta A_y}{A} \tag{5}$$

One capacitor consists of 31 fingers with a width of 60 µm and a length of 5950 µm, the connecting bridge has an area of 1.22 µm^2, the distance between the two electrodes is presumed at 40 µm and the dielectric constant of PDMS is taken as 2.5 [7]. A theoretical modeling of our sensor is shown in Figure 4.

For a normal force, an increase in all four capacitors is expected according to (5) since the dielectric spacer is then compressed. Figure 4(a) shows a slightly above-linear relation between the reduction of the distance between the parallel plates of the capacitor and the normalized change of capacitance. Figure 4(b) shows the four capacitance values for shear forces in x-direction. C_1 and C_3 change linearly in opposite directions with the displacement of the electrodes that lead to an increase and decrease in the overlapping area of the electrodes, respectively. The change of C_2 and C_4 is remaining zero as the overlapping area of these capacitors do not change. Similarly, for shear force in y-direction, C_2 and C_4 are increasing and decreasing, respectively, whereas C_1 and C_3 remain constant. A clear separation of the three force directions seems to be possible. However, a change in the normal force affects the change of the shown shear-force behavior.

Figure 5 highlights the influence of the normal displacement on the individual capacitor values. Previous work by Dobrzynka and Gijs [6] neglected this effect. However, already small normal forces that compress the dielectric layer by a few percent can lead to a large error, especially when measuring small shear forces. This work suggests calculating the C_x and C_y values according to (5) to reduce this effect.

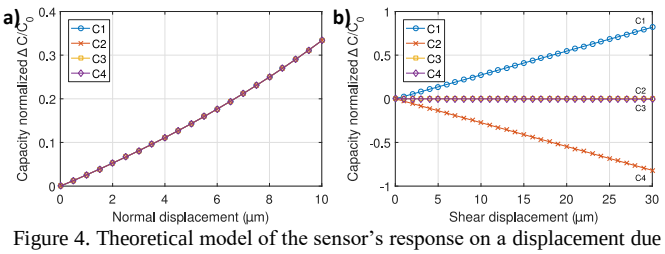

Figure 4. Theoretical model of the sensor's response on a displacement due to (a) normal force (z-direction) and (b) shear force in x direction.

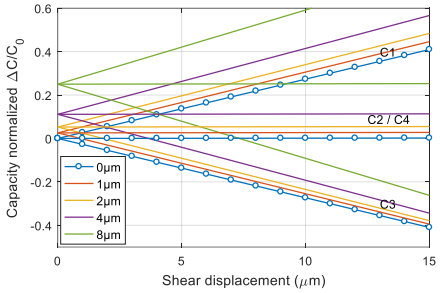

Figure 5. Calculated capacitance values for the individual capacitances for a shear load in x-direction at different constant z-forces.

C. Print Characterization

The silver ink printed on the PET film resulted in drops with a size of 60 µm, thus we chose a drop spacing of 30 µm to achieve a good line formation. Optical images of the printed electrodes in Figure 6 show a consistent pattern for two different finger widths of 60 µm and 210 µm. The printing of the very fine patterns proved to be too sensitive to nozzle failures that interrupt parts of the fingers. Furthermore, the alignment of the top and bottom electrodes turned out to be more difficult than initially assumed. So, we continued the work with the 210 µm fingers. The sensitivity is similar, but the total area of the sensor is increased.

The profile measurement shown in Figure 7 was recorded perpendicular to the printing direction. We measured an average thickness of 412 nm. The green markers indicate drop rows where nozzle failure occurred and the thickness of the film is much lower. Since these gaps only appear locally, we expect them to have a small influence on the conductivity of the electrodes. However, the thickness of the silver layer greatly affects the conductivity of the electrodes. At this point, we were not aware of the fact that the conductivity could be a problem for the performance of the sensor.

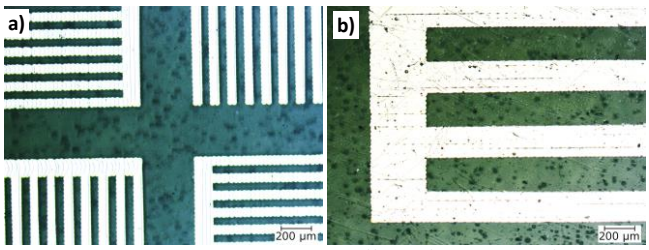

Figure 6. Inkjet printed electrodes with different finger width of (a) 60 µm and (b) 210 µm. The silver can be seen bright while the substrate is dark. The individual droplets form small bulges on the edges.

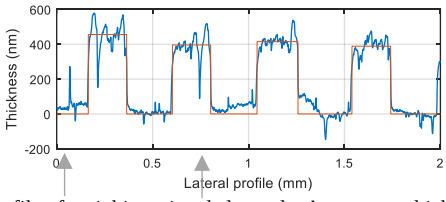

Figure 7. Profile of an inkjet-printed electrode. An average thickness of 412 nm was measured within the red marked areas. The spikes marked by green arrows may lead to an interruption of the conductive path.

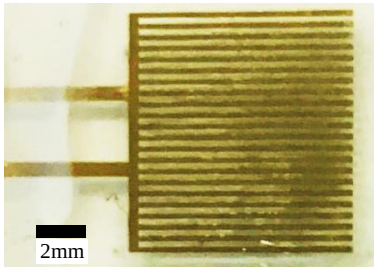

Figure 8. Optical image of one quarter of the sensor including wiring.

The fabricated sensor was then contacted at the rectangular contact-pads. Therefore, the overhanging PET foil was cut off and the contact-pads were uncovered. Figure 8 depicts the contacted sensor. To plug the sensor to the LCR meter, two small wires were attached by conductive epoxy.

D. Electro-Mechanical Characterization

The results of the normal force sensing experiments are depicted in Figure 9. The data is collected from a characterization cycle, including three rising and declining force ramps. The blue lines represent the reference force signal and the orange lines represent the capacity signal. In Figure 9(b), the solid line represents a shear force in -y-direction and the dashed lines a shear force in +y-direction. The sensor responses occur almost simultaneously with the application of a normal force.

Due to the viscoelastic relaxation of the PDMS, the capacitance during unloading of the force is slightly higher than at loading. Furthermore, a permanent part is remaining that takes more time to vanish. This viscoelastic behavior ismore pronounced for shear forces, for which the capacitance signal shows a small delay to the force signal. Especially for the unloading, the capacity follows tens of seconds after the force signal. Again, a remaining part of the capacitance signal can be observed.

The response of the capacitance to different forces is investigated in the following. For all the following plots, the solid lines represent the loading of the sensor and the dashed lines show the unloading response. To minimize errors in measurements and reduce noise, the 16 capacity values which were measured immediately before a change in applied force have been considered in the analysis. Figure 10 shows that the response of the sensor is linear to the normal force, and it can be seen that the hysteresis is small. The sensitivity is approximately 5.2 fF/N, which is very small. The reason lies at the large area of the sensor. The area where the PDMS was printed is approximately 2.5 x 2.5 cm² large, so the maximal

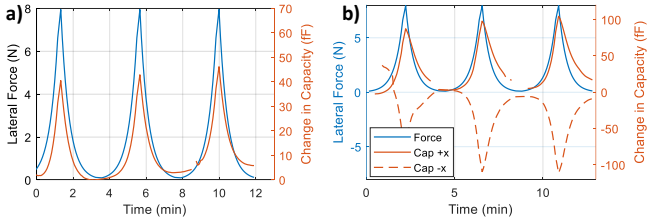

Figure 9. (a) Shows the capacity response (red) to a normal force (blue) over time. In (b) the solid red line corresponds to the capacitance change due to a force in –x-direction and the dashed line to the +x-direction.

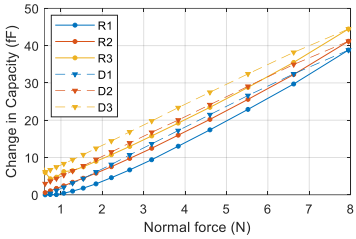

Figure 10. Characteristic of the sensor to three increasing (R, solid) and decreasing (D, dashed) cycles of normal force. A linear behavior was found. The drift of the signal can be explained by viscoelastic behavior of the PDMS and is reversed after a longer resting time.

pressure was only about 12.8 kPa. Thus, the sensitivity to pressure is about 3.25 fF/kPa.

Figure 11 shows the shear force response of the sensor for the two opposite shear directions. The shear response shows a symmetry for the two opposite directions, since the area of the capacitor is equally reduced or increased for a certain force. The slope of both curves is linear over the whole force range. Thus, the sensor is very close to the theoretical model. Thus, it can be seen that a positive or negative force results in the same absolute change in capacity. We measured a large hysteresis that is most probably related to the mechanical properties of the PDMS spacer. Due to the design of the sensor, its response for shear forces is considerably better than for normal forces. The sensitivity lies between 12.3 fF/N and 13.8 fF/N. Comparing our sensor to the sensitivity values of Dobrzynska and Gijs [4], we came very close to their results for the shear response while our sensor was three times less sensitive to normal forces (about 11 fF/kPa [4]).

The capacity values of the sensors are considerably lower than the theoretical values. From the profilometer measurement, we know that the thickness of the PDMS layer is about 40 µm and the area of the electrodes is about 44.4 mm^2. The theoretical capacity value for 50 % overlap is 12.3 pF. Our measured capacitance value was 6.82 pF and only half of the theoretical value. This capacitance would correspond to a distance of 96.8 µm. When checking the overlap of our sensor, we found that the overlap in resting state of about two thirds (67 %) was slightly higher than the desired value. This should lead to an even higher capacitance value of 16.5 pF. This significant deviation of the capacitance value originates most probably from some trapped air between the top electrode and the stencil-printed PDMS layer. Such trapped air bubbles are colored in red in Figure 12 and

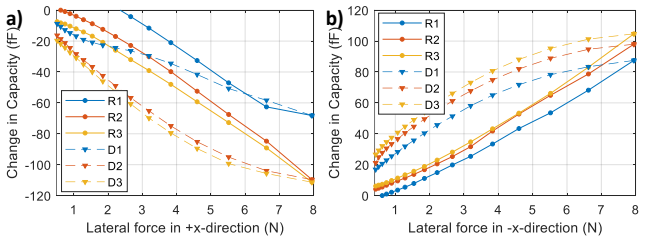

Figure 11. Characteristic of the sensor to three increasing (R) and decreasing (D) cycles of shear force in (a) +x direction and (b) –x direction. After the first force application, a linear behavior with a large hysteresis was found. The drift of the signal can be explained by viscoelastic behavior of the PDMS and is reversed after a longer resting time.

TABLE I: COMPARISON OF THE THEORETICAL AND MEASURED CAPACITY VALUES, THE THICKNESS OF THE DIELECTRIC SPACER D_0 AND THE DEFLECTION ΔD. BOLD VALUES ARE CALCULATED FROM THE OTHER COLUMNS.

	C_0 (pF)	Overlap	ε_r	d_0 (µm)	Δd (nm)
Ideal 50 %	**12.3**	50 %	2.5	40.0	**146**
Ideal 67 %	**16.5**	67 %	2.5	40.0	**109**
Sensor	6.82	67 %	2.5	**96.8**	**635**
S. (25 % air)	6.82	67 %	**1.8**	**69.7**	**457**

increase the average distance, but do not explain a factor of 2.5. Additionally, the lower relative permittivity of air (compared to PDMS) decreases the overall capacity. The trapped air acts like a second capacity connected in series. The capacity as a function of the fraction of air $\chi = d_2/d$ and $d = d_1 + d_2$ is:

$$C = \frac{\varepsilon_0 \varepsilon_r A}{d(1-\chi+\varepsilon_r \chi)} \quad (6)$$

Here, d is the total distance of the electrodes, d_1 denotes the thickness of the PDMS layer and d_2 is the thickness of the air gap. For example, if the spacer contains 25 % air and 75 % PDMS the capacity is reduced to 72.8 % of its ideal value ($\chi = 0$, no trapped air). The combination of the higher distance due to trapped air and a lower effective permittivity leads to a reasonable relation of capacitance and distance.

The change in capacitance is originated by a displacement Δd of the top electrode with respect to the bottom electrode. Using the distances in Table I, we calculated the change in distance for each of the four possibilities that results in the measured change in capacitance of about 45 fF. The range of the calculated distance changes of less than a micrometer is reasonable since PDMS has a Poisson's ratio of almost 0.5. Therefore, the PDMS is only little compressible as the lateral expansion is limited.

IV. CONCLUSIONS

In this work, a fully flexible, capacitive force sensor for two-axial force measurements has been developed by acquiring printed electronic technologies on a polymeric film. We successfully fabricated structured silver-based electrodes on PET foil by inkjet printing. We achieved a resolution with lines below 60 µm and an average thickness of about 500 nm. For a conducting layer, the inkjet-printed samples required an additional post-production treatment. With photonic sintering, an ultra-fast, selective, and cheap method was used to

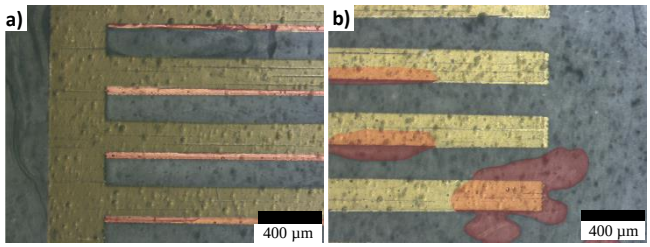

Figure 12. (a) Overlapping area of the electrodes colored in red onto an optical microscope picture and (b) trapped air in the PDMS layer colored in red as well for better visibility.

 ISBN: 978-1-61208-621-7

functionalize the thin-films. PDMS, which was chosen for its good processability and elastic properties, was found unsuitable for direct inkjet printing. Oxygen plasma treatment could be an effective way to overcome the hydrophobic surface properties of PDMS. But further research is required here. The most challenging task was to fabricate the stacked structure of a printed bottom electrode, a dielectric spacer, and a printed top electrode. The method of gluing the two printed sheets together to solve the problem was the best available. The main objective of this report to fabricate a printed normal and shear force sensor was achieved. By integrating this sensor into a 2-by-2 arrangement of four sensors, simultaneous normal and shear forces (three-axial) can be measured. Due to trapped air in the dielectric spacer, the experimental capacitive values were distinctly lower than the theoretical predictions.

The shear force response was characterized using a self-made setup, which was developed to minimize parasitic normal forces when exerting shear forces. The sensor exhibits a linear response to exerted shear and normal forces, operating in a range of 100 - 8000 mN. Under shear load operation the sensor shows hysteresis effects which can be ascribed to the mechanical properties of the PDMS layer. Through the design of the sensor, the sensitivity for shear forces was about twice that for normal forces. We calculated a shear force sensitivity of around S_x = 13.1 fF/N and a normal force sensitivity of S_z = 5.2 fF/N. All of the materials and methods used here are low-cost and cause a very small amount of chemical waste, especially when compared to conventional semiconductor processes.

ACKNOWLEDGMENT

This work was partially supported by the Deutsche Forschungsgemeinschaft (DFG) within the German Excellence Initiative through the cluster of excellence “Nanosystems Initiative Munich” (NIM) and the TUM Graduate School. The authors want to thank Prof. Cheng of the Technical University of Munich (TUM) for the use of their lab to produce the inkjet-printed patterns used in this work.

REFERENCES

[1] E.-S. Hwang, J. Seo, and Y.-J. Kim, “A Polymer-Based Flexible Tactile Sensor for Both Normal and Shear Load Detections and Its Application for Robotics,” *J. Microelectromechanical Syst.*, vol. 16, no. 3, pp. 556–563, Jun. 2007.

[2] R. S. Dahiya, G. Metta, M. Valle, and G. Sandini, “Tactile sensing-from humans to humanoids,” *IEEE Trans. Robot.*, vol. 26, no. 1, pp. 1–20, 2010.

[3] A. Albrecht, A. Rivadeneyra Torres, J. F. Salmerón, A. Abdellah, and P. Lugli, “Inkjet Printing and Photonic Sintering of Silver and Copper Oxide Nanoparticles for Ultra-Low-Cost Conductive Patterns,” *J. Mater. Chem. C*, Mar. 2016.

[4] T. A. T. A. Chase and R. C. R. C. Luo, “A thin-film flexible capacitive tactile normal/shear force array sensor,” in *Proceedings of IECON ’95 - 21st Annual Conference on IEEE Industrial Electronics*, 1995, vol. 2, pp. 1196–1201.

[5] S. Khan, L. Lorenzelli, and R. S. Dahiya, “Screen printed flexible pressure sensors skin,” *ASMC (Advanced Semicond. Manuf. Conf. Proc.*, pp. 219–224, 2014.

[6] J. A. Dobrzynska and M. A. M. Gijs, “Polymer-based flexible capacitive sensor for three-axial force measurements,” *J. Micromechanics Microengineering*, vol. 23, no. 1, p. 15009, Jan. 2013.

[7] J. E. Mark, *Polymer data handbook*. Oxford University Press, 2009.

 ISBN: 978-1-61208-621-7